Available online at www.sciencedirect.com

SCIENCE DIRECT

Developmental Biology 282 (2005) 361 – 373

DEVELOPMENTAL BIOLOGY

www.elsevier.com/locate/ydbio

Gene knockout analysis of two γ-tubulin isoforms in mice

Akiko Yuba-Kubo[a], Akiharu Kubo[a,b], Masaki Hata[c], Shoichiro Tsukita[a,b,*]

[a]*Solution Oriented Research for Science and Technology, Japan Science and Technology, Corporation, Sakyo-ku, Kyoto 606-8501, Japan*
[b]*Department of Cell Biology, Faculty of Medicine, Kyoto University, Sakyo-ku, Kyoto 606-8501, Japan*
[c]*KAN Research Institute, Kyoto Research Park, Shimogyo-ku, Kyoto 600-8815, Japan*

Received for publication 12 November 2004, revised 14 March 2005, accepted 16 March 2005
Available online 11 May 2005

Abstract

γ-Tubulin regulates the nucleation of microtubules, but knowledge of its functions in vivo is still fragmentary. Here, we report the identification of two closely related γ-tubulin isoforms, TUBG1 and TUBG2, in mice, and the generation of TUBG1- and TUBG2-deficient mice. TUBG1 was expressed ubiquitously, whereas TUBG2 was primarily detected in the brain. The development of TUBG1-deficient (*Tubg1*$^{-/-}$) embryos stopped at the morula/blastocyst stages due to a characteristic mitotic arrest: the mitotic spindle was highly disorganized, and disorganized spindles showed one or two pole-like foci of bundled MTs that were surrounded by condensed chromosomes. TUBG2 was expressed in blastocysts, but could not rescue the TUBG1 deficiency. By contrast, TUBG2-deficient (*Tubg2*$^{-/-}$) mice were born, grew, and intercrossed normally. In the brain of wild-type mice, TUBG2 was expressed in approximately the same amount as TUBG1, but no histological abnormalities were found in the *Tubg2*$^{-/-}$ brain. These findings indicated that TUBG1 and TUBG2 are not functionally equivalent in vivo, that TUBG1 corresponds to conventional γ-tubulin, and that TUBG2 may have some unidentified function in the brain.

Keywords: γ-Tubulin; Microtubule; Isoform; Gene knockout; Mitotic spindle

Introduction

γ-Tubulin was initially identified as a suppressor of a β-tubulin mutation in *Aspergillus nidulans* (Oakley and Oakley, 1989) and is now categorized as a member of the tubulin superfamily (for reviews, see Burns, 1995; Joshi, 1994; Oakley, 2000; Oakley and Akkari, 1999). Evidence accumulated from a variety of genetic and biochemical experiments has shown that γ-tubulin plays a central role in the nucleation of microtubules (MTs) (Oakley et al., 1990; Stearns and Kirschner, 1994; Zheng et al., 1991; for reviews, see Moritz and Agard, 2001; Oakley, 2000; Schiebel, 2000). This γ-tubulin-based MT nucleation system has been found in various species of animals and plants (reviewed in Gunawardane et al., 2000a; Oakley and Akkari, 1999). In *Drosophila* and *Xenopus*, γ-tubulin forms a huge macromolecular complex, a characteristic ring structure ~25 nm in diameter, which is called the γ-tubulin ring complex (γTuRC), together with various γ-tubulin ring proteins (Gunawardane et al., 2000b; Moritz et al., 1995, 1998; Oegema et al., 1999; Zheng et al., 1995; reviewed in Gunawardane et al., 2000a; Job et al., 2003; Moritz and Agard, 2001; Schiebel, 2000; Wiese and Zheng, 1999). Within the cell, γ-tubulin is concentrated at centrosomes as γTuRC, but it is also distributed in the cytoplasm as a soluble pool (Daunderer and Graf, 2002; Moudjou et al., 1996). The centrosome is the primary site where the MT nucleation occurs, and centrosomal γTuRC is thought to be responsible for this nucleation process as well as the anchoring of MT minus ends to centrioles (Dictenberg et al., 1998; Doxsey et al., 1994; Joshi, 1994; Mogensen et al., 2000; Moritz et al., 1998; Schnackenberg et al., 1998; Takahashi et al., 2002; Vogel et al., 1997; Wu and Palazzo, 1999; Zheng et al., 1995; Zimmerman et al., 2004). The function of the cytoplasmic γ-tubulin remains unclear, but

* Corresponding author. Department of Cell Biology, Faculty of Medicine, Kyoto University, Konoe-Yoshida, Sakyo-ku, Kyoto 606-8501, Japan. Fax: +81 75 753 4660.
E-mail address: htsukita@mfour.med.kyoto-u.ac.jp (S. Tsukita).

0012-1606/$ - see front matter © 2005 Elsevier Inc. All rights reserved.
doi:10.1016/j.ydbio.2005.03.031

one possibility is that this cytoplasmic γ-tubulin caps MT minus ends to modify their dynamics (Wiese and Zheng, 2000).

Interestingly, in various evolutionarily diverse organisms such as *Arabidopsis thaliana* (Liu et al., 1994), *Zea mays* (Lopez et al., 1995), *Physarum polycephalum* (Lajoie-Mazenc et al., 1996), *Euplotes crassus* (Tan and Heckmann, 1998), *Paramecium tetraurelia* (Ruiz et al., 1999), *Drosophila melanogaster* (Wilson et al., 1997), and humans (Wise et al., 2000), two (or three) isoforms were identified for γ-tubulin. However, neither their phylogenetic evolution nor the isoform-specific expression/function has been well characterized. In *Drosophila*, however, the isoform-specific expression of γ-tubulin has been examined especially during gametogenesis and development. One isoform was located in chromosome region 37C and its expression was restricted to ovaries and precellular embryos. By contrast, the other isoform was located at 23C and was expressed in somatic tissues and testes (Tavosanis et al., 1997; Wilson et al., 1997). Among vertebrates, only in humans has the existence of two closely related γ-tubulin genes, TUBG1 and TUBG2, been reported (Wise et al., 2000).

Phenotypic changes associated with the suppression of γ-tubulin expression have been examined in *A. nidulans*, *Saccharomyces pombe*, *Saccharomyces cerevisiae*, *Caenorhabditis elegans*, and *D. melanogaster* (Hannak et al., 2002; Horio et al., 1991; Marschall et al., 1996; Oakley et al., 1990; Spang et al., 1996; Sobel and Snyder, 1995; Stearns et al., 1991; Strome et al., 2001; Sunkel et al., 1995; Tavosanis et al., 1997; Wilson and Borisy, 1998), but knowledge of the in vivo functions of γ-tubulin in vertebrates is still lacking. Furthermore, the physiological relevance of the existence of two γ-tubulin isoforms is far from understood. As a first step to addressing these issues, in this study, we identified mouse orthologs of TUBG1 and TUBG2, and generated mice lacking the ability to express TUBG1 or TUBG2. We report here the phenotypes of these mice and discuss the in vivo functions of γ-tubulin isoforms in mice.

Materials and methods

Antibodies and cells

Rabbit anti-γ-tubulin pAb, mouse anti-γ-tubulin mAb (GTU-88), mouse anti-α-tubulin mAb (DM1A), Cy3-conjugated mouse anti-β-tubulin mAb (TUB2.1), and FITC-conjugated mouse anti-α-tubulin mAb (FITC-DM1A) were purchased from Sigma. Mouse anti-pericentrin mAb (BD-611814) and mouse anti-FLAG tag mAb were purchased from BD Biosciences (Franklin Lakes, NJ) and Stratagene (La Jolla, CA), respectively.

Mouse Eph4 epithelial cells were cultured in Dulbecco's modified Eagle's medium supplemented with 10% fetal calf serum.

Cloning of mouse TUBG1 and TUBG2 cDNAs and transfection

A 424-bp fragment corresponding to nucleotides 881–1304 of human TUBG1 (Zheng et al., 1991) was amplified by PCR and was used as a probe to screen a mouse lung λZAPII cDNA library (Stratagene): one clone (pTUBG1) contained a 1.6-kb insert including a full-length ORF (1353 bp) of mouse TUBG1. TUBG2 cDNA was cloned from the ES cell line (J1) by RT-PCR using the primer pair 5′-gctaggtctgatcggcgatgccc-3′ (forward)/5′-caatgcatcatcacgcttt-tat-3′ (reverse).

TUBG1 and TUBG2 were tagged with FLAG-peptide at their COOH termini basically according to a method described previously (Furuse et al., 1998). To construct expression vectors for FLAG-TUBG1 (pCTUBG1-F) and FLAG-TUBG2 (pCTUBG2-F), an *Eco*RI site was introduced at the stop codon of *Tubg1* and *Tubg2* cDNAs by PCR, and these PCR fragments and an adapter DNA encoding a FLAG peptide were introduced into pCAGGS-neodel*Eco*RI (Niwa et al., 1991), provided by Dr. J. Miyazaki (Osaka University). Cultured Eph4 epithelial cells were transfected with these expression vectors under a low Ca^{++} concentration (50 μM) condition using LipofectAmine Plus (GIBCO BRL, Gaithersburg, MD), as described previously (Furuse et al., 1998). After 2-week culture in the presence of 400 μg/ml of G418, resistant colonies were removed, and the clones expressing tagged proteins were screened by fluorescence microscopy with anti-FLAG mAb.

Phylogenetic tree

The UPGMA tree for γ-tubulins was constructed using the PROTDIST and NEIGHBOR programs contained in the Phylogeny Inference Package (PHYLIP, ver. 3.6a; Felsenstein, 2003). The following amino acid sequences were used: Arabidopsis TUBG1, *Arabidopsis thaliana* NP_191724; Arabidopsis TUBG2, *Arabidopsis thaliana* NP_196181; *Zea mays* TUBG1, *Zea mays* Q41807; *Zea mays* TUBG2, *Zea mays* Q41808; Paramecium, *Paramecium tetraurelia* CAA09991; Danio rerio, *Danio rerio* NP957202; Xenopus, *Xenopus laevis* M63446; Human TUBG1, *Homo sapiens* NP_001061; Human TUBG2, *Homo sapiens* NP_057521; Chimpanzee TUBG1, *Pan troglodytes* ENSPTRT00000016945; Chimpanzee TUBG2, *Pan troglodytes* ENSPTRT00000016947; Mouse TUBG1, *Mus musculus* BAD27264 (this study); Mouse TUBG2, *Mus musculus* BAD27265 (this study); Magnaporthe, *Magnaporthe grisea 70-15* XP_368283; Neurospora, *Neurospora crassa* XP_323273; Fission yeast, *Schizosaccharomyces pombe* NP_596147; Sea urchin, *Strongylocentrotus purpuratus* NP_999657; Drosophila TUB23C, *Drosophila melanogaster* CG3157-PA; Drosophila TUB37C, *Drosophila melanogaster* CG17566-PA; Chlamydomonas, *Chlamydomonas reinhardtii* U31545.

Generation of Tubg1$^{-/-}$ and Tubg2$^{-/-}$ mice

To generate *Tubg1*$^{-/-}$ mice, we screened a 129/Sv genomic library using pTUBG1 as a probe and obtained two overlapping clones containing the *Tubg1* gene. The targeting vector was then constructed as shown in Fig. 2A. An enhancer of engrailed-2 (En2)/splicing acceptor (SA), an internal ribosomal binding site (IRES), a β-galactosidase (lacZ) gene, a neomycin-resistance gene, and a polyadenylation signal (Niwa et al., 2000) were placed between a 1.6-kb 5′ arm and 5.4-kb 3′ arm. This targeting vector was designed to delete most of exons1, 2, and 3. J1 embryonic stem (ES) cells were electroporated with the targeting vector and selected for ~9 days in the presence of G418 as described previously (Shibata et al., 1997). The G418-resistant colonies were removed and screened by Southern blotting with the 5′ external probes. When the genomic DNAs were digested with *Sac*I, correctly targeted ES clones (clone 16 and 33) were identified by an additional 5-kb band together with the 7-kb band of the wild-type allele with the 5′ probe.

To generate *Tubg2*$^{-/-}$ mice, we screened a 129/Sv genomic library using pTUBG1 as a probe and obtained two overlapping clones containing the *Tubg2* gene. The targeting vector was then constructed as shown in Fig. 4A. A pgk-neo cassette was placed between a 1.3-kb 5′ arm and 6.2-kb 3′ arm. This targeting vector was designed to delete exon5 of *tugb2* by replacing it with the pgk-neo cassette. Electroporation and screening were performed as mentioned above. When the genomic DNAs were digested with *Hin*cII, correctly targeted ES clones (clone 47 and 490) were identified by an additional 5.0-kb band together with the 2.0-kb band of the wild-type allele with the 5′ probe.

Targeted ES cells obtained were injected into C57BL/6 blastocysts, which were in turn transferred into ICR foster mothers to obtain chimeric mice. Male chimeras were mated with C57BL/6J females, and agouti offsprings were genotyped to confirm the germ line transmission of the targeted allele. The littermates were genotyped by Southern blotting. Heterozygous mice were then interbred to produce homozygous mice.

Recovery of embryos at preimplantation stage and in vitro culture

Females were paired with males overnight and checked for vaginal plugs the next morning. Early embryos including 8-cell embryos were recovered from the oviduct by perfusing M2 medium containing 4 mg/ml of bovine serum albumin (M2 + BSA; Fulton and Whittingham, 1978) and cultured on a glass-bottomed dish with a cover glass (No.1S, Matsunami) for 2 days at 37°C under a CO_2 atmosphere in the presence or absence of 1 μM SYTO16 (Molecular Probes, Eugene). Nuclear divisions were followed under a conventional fluorescence microscope. Images of embryos at each stage were acquired with a DeltaVision optical sectioning microscope (Version 2.00; Applied Precision Inc.) equipped with an Olympus IX70 (PlanApo 60×/1.40 NA or PlanApo 100×/1.40 NA oil immersion objective) microscope.

Northern blotting

The expression of TUBG1 and TUBG2 in various mouse tissues was examined by Northern blotting using Mouse Multiple Tissue Northern Blot (Clontech, CA). Hybridization with DIG-labeled probes was performed according to the manufacturer's directions (Roche). Probes were amplified from the 3′-untranslated regions of TUBG1 and TUBG2 cDNAs using the following primer pairs: 5′-gtcacggacgacagggac-3′ (forward)/5′-tggtttacatccagtgctttat-3′ (reverse) and 5′-cctggacaagaagcacagc-3′ (forward)/5′-caatgcatcatcacgctttat-3′ (reverse), respectively.

Immunoblotting

The heart, brain, liver, kidney, and testis were dissected from adult mice, minced, homogenized in SDS sample buffer (Laemmli, 1970), and then boiled for 10 min. Blastocysts were washed three times with M2 medium supplemented with 4 mg/ml of polyvinyl-pyrrolidone and collected in a small drop of the same solution. They were then mixed with an equal volume of ×2 concentrated SDS sample buffer and boiled 2 min. These boiled samples were separated electrophoretically in SDS–polyacrylamide gels (12.5% acrylamide and 0.083% *N*,*N*′-methylene-bisacrylamide) and transferred onto Immobilon transfer membranes (Millipore). Membranes were then incubated with mouse anti-γ-tubulin mAb (GTU-88) and bound antibodies were detected with HRP-conjugated anti-mouse IgG (Amersham) and ECL plus detection kit (Amersham).

Immunofluorescence microscopy

Blastocysts that were developed in vitro were washed with PBS and fixed with 3.7% formaldehyde in PBS at 37°C for 10 min. They were washed 3 times with PBS for 5 min and permeabilized with PBS containing 0.2% Tween 20 for 5 min. After being rinsed in PBS twice, they were incubated with a blocking solution, DMEM containing 20% fetal calf serum (FCS/DMEM). They were incubated with primary antibodies in FCS/DMEM for 2 h, washed with FCS/DMEM several times, and then incubated with secondary antibodies for 2 h. As secondary antibodies, Alexa Flour 488-conjugated anti-mouse IgG (A-11029) and Alexa Fluor 594-conjugated anti-rabbit IgG (A-11032) were used. After being washed with PBS, samples were mounted in Mowiol (Calbiochem) and observed under a DeltaVision optical sectioning microscope.

In situ hybridization

In situ hybridization analysis was performed on paraffin sections of mouse brain (Novagen). The TUBG2-specific DIG-labeled RNA probe was synthesized from a Northern blot probe as described previously (Komiya et al., 1997). Brain paraffin sections were de-waxed and pretreated with solution A [5 × SSC (pH 4.5), 50% formamide, and 1% SDS] containing 50 μg/ml of yeast tRNA and 50 μg/ml of heparin for 2 h at 60°C. Each section was then hybridized with 50 μl of solution A containing 1 μg/ml of DIG-labeled RNA probe overnight in a moist chamber. Hybridized sections were washed once with solution A for 10 min at room temperature, twice with 5 × SSC/50% formamide for 30 min at 60°C, three times with 2 × SSC/50% formamide for 30 min at 60°C, and once with MalST [0.1 M maleic acid, 0.15 M NaCl, 0.1% Tween 20 (pH 7.0)] for 10 min at room temperature. Hybridized probes on sections were detected immunologically: sections were labeled with anti-DIG-POD antibody (×100; Roche), which was localized using the TSA biotin system (NEL700A, NEN) followed by incubation with 45 mM Tris–HCl buffer (pH 7.5) containing 0.05% diaminobenzidine and 0.005% H_2O_2 for 30 min at room temperature. Sections were counterstained with hematoxylin, dehydrated with an ethanol/xylene series, and mounted in Biolite (Ohken Tokyo, Japan). Photographs were taken by Axioplan with a 40× Plan-apochromat (Zeiss).

Results

Identification of two closely related γ-tubulin isoforms, Tubg1 and Tubg2, in mice

During the course of cloning γ-tubulin cDNA from various mouse tissues, we noticed that there are two distinct isoforms of γ-tubulin (accession nos. AB158480 and AB158481). Sequencing of the cDNAs revealed that these two isoforms are very similar in amino acid sequence, showing 96.9% identity. Among 451 amino acid residues, only 15 differed, with most changes in the COOH-terminal region (Fig. 1A). These γ-tubulin genes were located on mouse chromosome 11D in tandem. In good agreement, in humans, two distinct, but closely related, γ-tubulin isoforms, TUBG1 and TUBG2, were previously identified at 17q21 in tandem (Wise et al., 2000). Close comparison of the genomic information for these γ-tubulin genes indicated that the mouse γ-tubulin genes identified here are orthologs of human TUBG1 and TUBG2 (data not shown). At the amino acid sequence level, mouse TUBG1 and TUBG2 showed 98.9% and 96.9% identity to the corresponding human γ-tubulin isoforms, respectively. Moreover, in both mouse and human, the TUBG1 and TUBG2 genes shared the same intron/exon organization, suggesting that the two genes arose from the duplication of a common ancestor. Phylogenetic analysis revealed that this duplication occurred very recently, independently from *Drosophila* γ-tubulin duplication (Fig. 1B).

We then designed Northern blot probes specific for mouse TUBG1 and TUBG2 using their 3′-noncoding regions and examined their tissue expression patterns (Fig. 1C). TUBG1 mRNA bands (~1.6 kb) were detected in all the tissues examined though expression levels varied significantly depending on the tissues, whereas the TUBG2 mRNA (~1.6 kb) band was detectable primarily in the brain: with overexposure for autoradiography, TUBG2 mRNA was detected faintly also in the heart, liver, kidney, and testis. In human, the expression of TUBG2 was reported to be detected in various organs by RT-PCR (Wise et al., 2000), and consistently, also in mice, TUBG2 mRNA was widely detectable at the detection level of RT-PCR (data not shown).

We made an effort to generate antibodies that can distinguish TUBG1 and TUBG2, but failed to obtain such specific antibodies. Therefore, we exogenously expressed FLAG-tagged TUBG1 or TUBG2 in cultured mouse epithelial cells (Eph4 cells) and stained stable transfectants with anti-FLAG mAb (Fig. 1D). Interestingly, both FLAG-tagged TUBG1 and TUBG2 were concentrated at centrosomes in interphase as well as mitotic cells, and no difference was discerned in their subcellular localization.

Tubg1-deficient mice; defects in mitosis in early embryos

As a first step towards understanding the physiological relevance of the existence of two similar γ-tubulin isoforms in mice, we produced mice unable to express TUBG1. Nucleotide sequencing as well as restriction mapping identified eleven exons that cover the whole open reading frame of *Tubg1*: exon 1 contained the first ATG (Fig. 2A). We constructed a targeting vector, which was designed to disrupt *Tubg1* in ES cells by replacing most of exon 1/2/3 with the neomycin resistance gene. Correctly targeted ES cells were selected by Southern blotting with a 5′ probe and a neo probe, and two ES cell clones (clone 16 and 33), in which one of the *Tubg1* alleles was disrupted by homologous recombination, were obtained.

Then, two lines of heterozygous mutant ($Tubg1^{+/-}$) mice were generated separately from clones 16 and 33 (Fig. 2B). These $Tubg1^{+/-}$ mice appeared indistinguishable from wild-type ($Tubg1^{+/+}$) mice. Offsprings analyzed from matings of $Tubg1^{+/-}$ mice were either $Tubg1^{+/-}$ or $Tubg1^{+/+}$ in genotype (Table 1), suggesting that mice heterozygous for the *Tubg1* allele developed normally. In support of these findings, a histological analysis of newborn $Tubg1^{+/-}$ mice revealed no obvious defects. The data also suggested that homozygous mutant ($Tubg1^{-/-}$) mice died before birth. On investigating $Tubg1^{-/-}$ embryonic lethality further, we found that $Tubg1^{+/-}$ matings produced no $Tubg1^{-/-}$

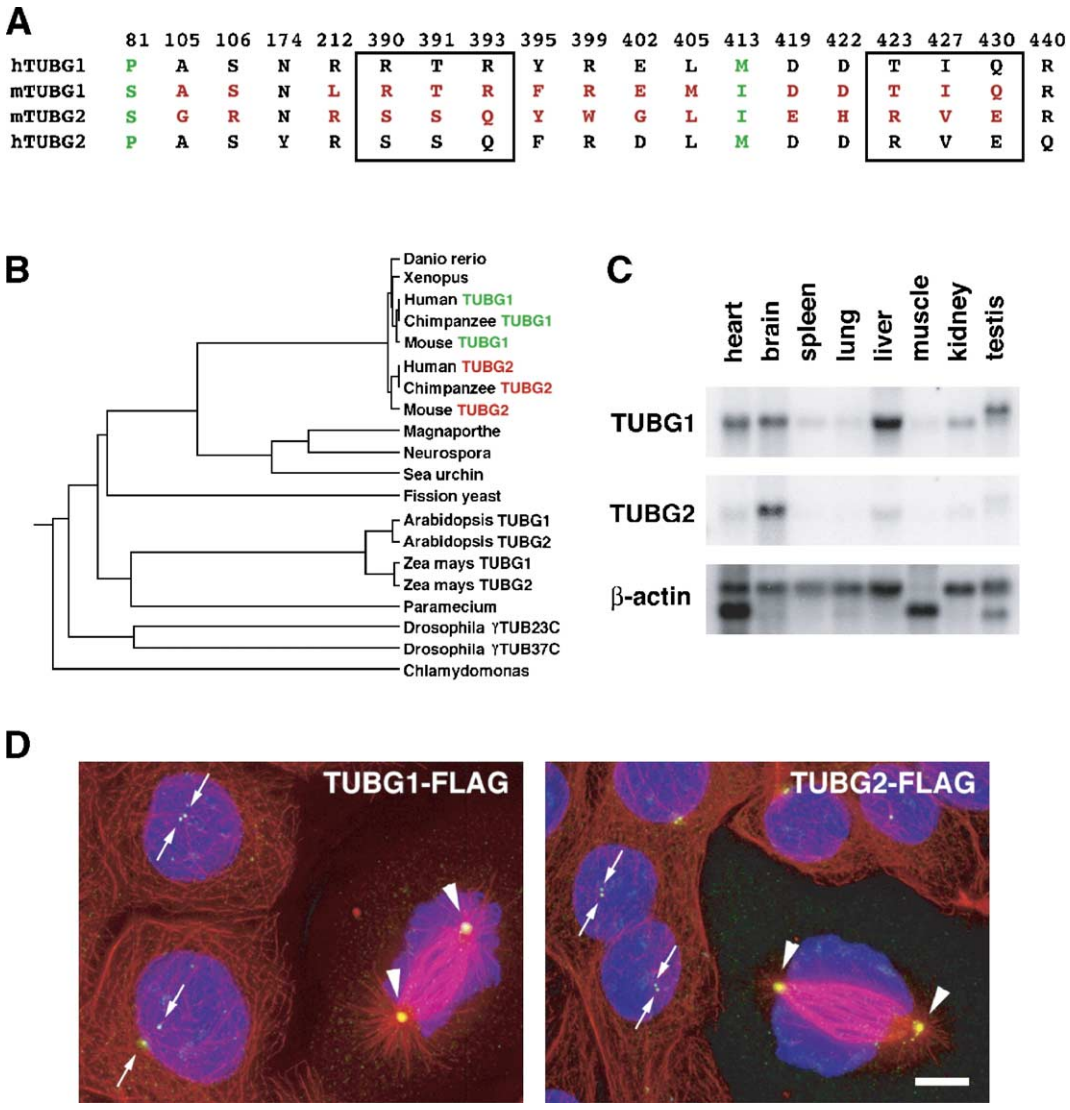

Fig. 1. Two closely related γ-tubulin isoforms in mice. (A) Comparison of the deduced amino acid sequences between human and mouse γ-tubulin isoforms: the accession numbers of the amino acid sequence of human TUBG1, mouse TUBG1, human TUBG2, and mouse TUBG2 are NP_001061, BAD27264, NP_057521, and BAD27265, respectively. Among 451 amino acid residues, only 19, which are shown with amino acid location numbers, are not conserved. The 15 amino acid residues represented in red differ between mouse TUBG1 and mouse TUBG2, 12 of which are located in the COOH-terminal region. Amino acid residues conserved in a human- or mouse-specific manner are colored green. Amino acid residues conserved in a TUBG1- or TUBG2-specific manner are clustered in two boxed regions. (B) Phylogenetic tree of γ-tubulins calculated with the program UPGMA. Duplication of the γ-tubulin gene in mouse/human appears to have occurred independently from that in *Drosophila*. (C) Northern blots of TUBG1 and TUBG2 expression in various mouse tissues. Mouse multiple tissue Northern blot (Clontech) was probed with DNA fragments corresponding to 3′ noncoding flanking regions of TUBG1 and TUBG2. β-Actin probe was used as a control. TUBG1 mRNA (~1.6 kb) was detected ubiquitously though its expression level varied depending on the tissues. By contrast, TUBG2 mRNA (~1.6 kb) was detected primarily in the brain. (D) Subcellular localization of exogenously expressed FLAG-tagged TUBG1 and TUBG2 in mouse Eph4 cells. Cells fixed with cold methanol were triple-stained with anti-FLAG mAb (green), Cy3-conjugated anti-β-tubulin mAb (red), and DAPI (blue). TUBG1 and TUBG2 were concentrated at centrosome not only in interphase cells (arrows) but also in mitotic cells (arrowheads). Scale bar, 5 μm.

embryos at any stage after gastrulation (data not shown). These results indicated that the targeting of both *Tubg1* alleles gave rise to early embryonic lethality in mice. Then, we performed genotype analyses of $Tubg1^{+/-}$ intercross embryos at the preimplantation stage by PCR. Interestingly, both at the 8-cell (E2.5) (Fig. 2C) and early blastocyst stages (E3.5), $Tubg1^{-/-}$ embryos appeared to be alive (Table 1).

We then compared the in vitro development of embryos at the preimplantation stage between $Tubg1^{+/+}$ and $Tubg1^{-/-}$ embryos: $Tubg1^{+/-}$ intercross embryos were collected at the 8-cell stage from the oviduct and cultured for 2 days at 37°C under a CO_2 atmosphere in M16 medium that contained SYTO16 to vitally stain DNA. Nuclear divisions were pursued in live embryos by fluorescence microscopy. After observations, genomic DNA from each embryo was recovered to determine its genotype by PCR. During this 2-day culture, $Tubg1^{+/+}$ 8-cell embryos developed to blastocysts (128 cells) of normal appearance via the morula stage (Figs.

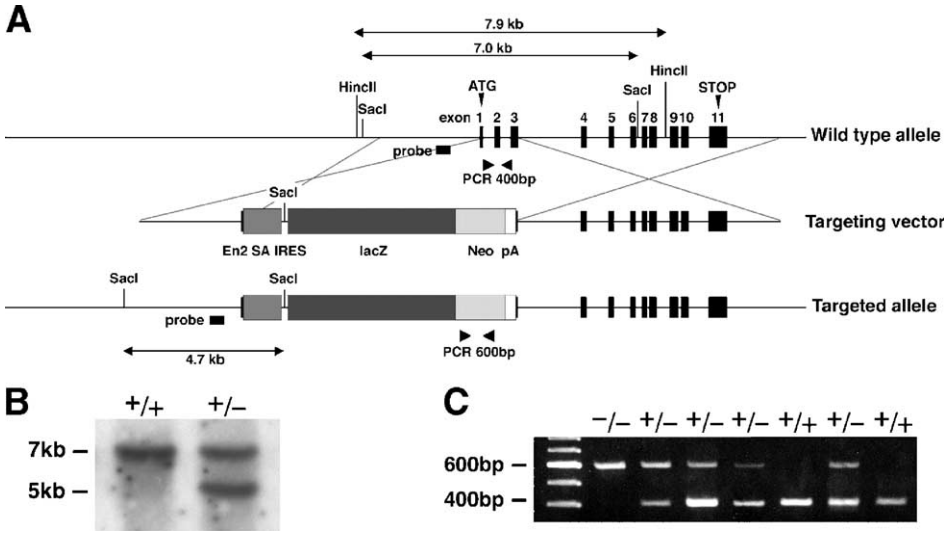

Fig. 2. TUBG1 gene knockout by homologous recombination in mice. (A) Restriction maps of the wild-type allele, the targeting vector, and the targeted allele of the mouse TUBG1 gene. Eleven exons (closed boxes) were identified, among which exon 1 contained the first ATG. The targeting vector contained an enhancer of engrailed-2 (En2)/splicing acceptor (SA), an internal ribosomal binding site (IRES), a β-galactosidase gene (lacZ), a neomycin-resistance gene (Neo), and a polyadenylation signal (pA) in this order in its middle portion to delete most of exons 1, 2, and 3. The position of the 5′ probe for Southern blotting is indicated as a bar. Arrowheads show PCR primers used for genotyping. (B) Genotype analyses by Southern blotting of *Sac*I-digested genomic DNA from 4-week-old wild-type (+/+) and heterozygous (+/−) mice for the mutant TUBG1 gene allele. Southern blotting with the 5′ probe yielded a 7.0-kb band from the wild-type allele and a 4.7-kb band from the targeted allele (see A). (C) Genotype analyses of E2.5 embryos (8-celll stage) obtained from $Tubg1^{+/-}$ matings. Genomic DNA was isolated from individual embryos, and genotypes were determined by PCR using primers described in A: these primers gave rise to 400-bp and 600-bp fragments from wild-type and targeted alleles, respectively.

3A, a and b): individual cells achieved normal cell divisions repeatedly. In contrast, when $Tubg1^{-/-}$ 8-cell embryos were cultured, at the morula stage (16–32 cells), several cells began to show clear defects in nuclear division. In these cells, the cell division was arrested with abnormally condensed/unaligned chromosomes. At the early blastocyst stage, these mitotic arrested cells increased in number, and finally, most cells in the $Tubg1^{-/-}$ blastocyst showed abnormally condensed/unaligned chromosomes (Figs. 3A, d and e). These findings indicated that the development of $Tubg1^{-/-}$ embryos stopped at the blastocyst stage due to mitotic arrest.

In order to further examine the process of mitotic arrest induced by TUBG1 deficiency, blastocysts were whole-mount stained with anti-α-tubulin mAb and DAPI. In $Tubg1^{+/+}$ blastocysts, most cells appeared to be at the interphase showing characteristic networks of MTs in the cytoplasm, and only a small number of cells bore mitotic spindles (Fig. 3A, c). Interestingly, in $Tubg1^{-/-}$ blastocysts, most cells showed abnormal deformed mitotic spindle-like structures, concomitantly carrying condensed/unaligned chromosomes, indicating that these cells were under prometaphase–metaphase arrest (Fig. 3A, f). We then whole-mount stained $Tubg1^{+/+}$ and $Tubg1^{-/-}$ blastocysts with anti-α-tubulin mAb, anti-pericentrin mAb (a centrosomal marker), and DAPI. In $Tubg1^{+/+}$ cells, pericentrin was concentrated at the poles of bipolar mitotic spindles (Fig. 3B, a). In $Tubg1^{-/-}$ cells, mitotic spindle-like structures were severely disorganized, although MTs themselves did not appear to be highly destabilized. The symmetrical feature of the spindle was frequently lost with one or two foci of bundled MTs that were surrounded by condensed chromosomes. Pericentrin-positive foci still remained in these cells, but there was only one focus for each cell: they were not associated with pole-like structures, though they were located in close proximity to MT bundles (Figs. 3B, b–f).

Table 1
Genotype analyses of the offsprings of heterozygous intercrosses

Isotypes	Age (ES clone)	Genotype		
		+/+	+/–	–/–
TUBG1	E2.5 (clone 16)	4	3	1
	E3.5 (clone 16)	14	41	7
	Post (clone 16)	57	82	0
	Post (clone 33)	6	12	0
TUBG2	Post (clone 490)	31	58	31

Tubg2-deficient mice; normal development, growth, and fertility

We next generated *Tubg2*-deficient mice ($Tubg2^{-/-}$). Similar to *Tubg1*, *Tubg2* contained 11 exons (Fig. 4A). We constructed a targeting vector, which was designed to disrupt *Tubg2* in ES cells by replacing exon 5 with the neomycin resistance gene. Correctly targeted ES cells were selected by Southern blotting with a 5′ probe and a neo probe, and ES cell clones, in which one of the *Tubg2* alleles was disrupted by homologous recombination, were obtained. Then, one line of heterozygous mutant ($Tubg2^{+/-}$) mice was generated.

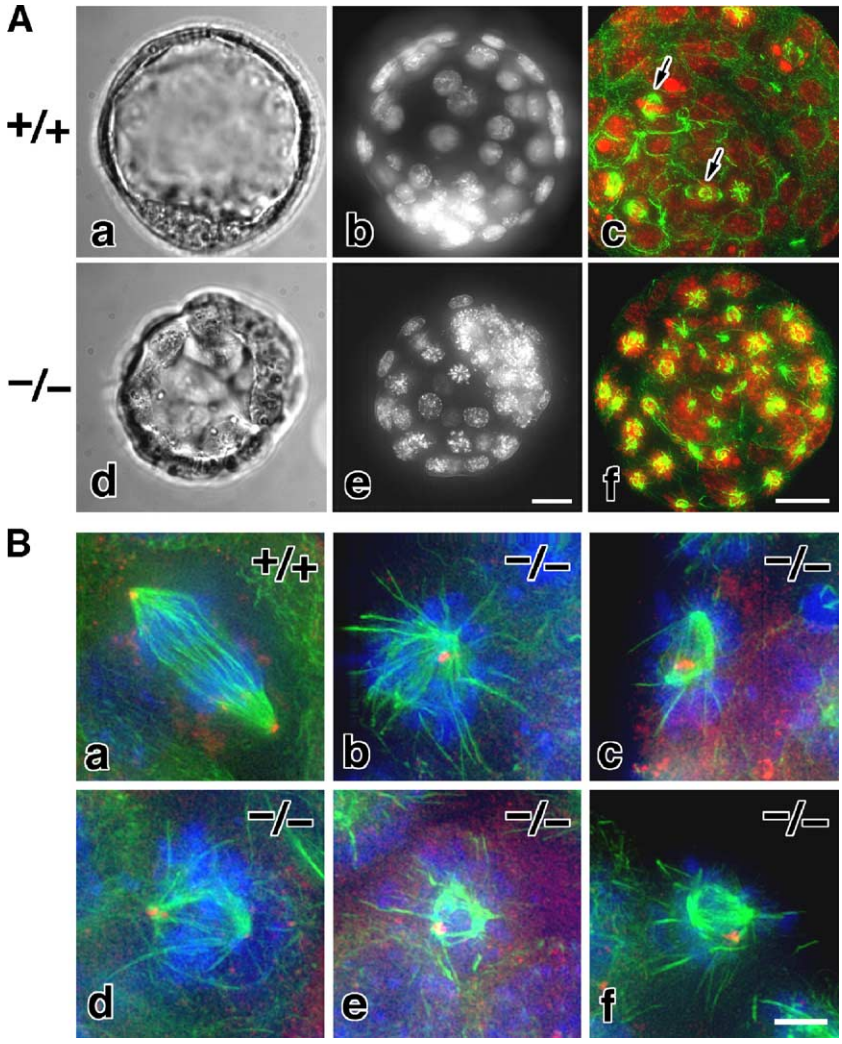

Fig. 3. Mitotic defects in *Tubg1*$^{-/-}$ embryos at the blastocyst stage. (A) Live and fixed images of *Tubg1*$^{+/+}$ (a–c) and *Tubg1*$^{-/-}$ (d–f) blastocysts. *Tubg1*$^{+/-}$ intercross embryos were collected at the 8-cell stage from the oviduct and cultured for 2 days at 37°C under a CO_2 atmosphere in M16 medium that contained SYTO16 to vitally stain DNA. After live observations by phase contrast microscopy (a and d) and fluorescence microscopy (b and e), embryos were genotyped. During the 2-day culture, *Tubg1*$^{+/+}$ 8-cell embryos repeated cell divisions and developed to blastocysts (a) with normal appearing nuclei (b). By contrast, in *Tubg1*$^{-/-}$ embryos, mitotic arrest began to be observed at the morula stage, and at the blastocyst stage (d), most cells showed abnormally condensed/unaligned chromosomes (e). When blastocysts were fixed with 3.7% formaldehyde and whole-mount stained doubly with anti-α-tubulin mAb (green) and DAPI (red pseudocolor), most cells in *Tubg1*$^{+/+}$ blastocysts appeared to be at the interphase showing characteristic MT networks in the cytoplasm, and only a small number of cells (arrows) bore mitotic spindles (c). By contrast, in *Tubg1*$^{-/-}$ blastocysts (f), most cells showed abnormal deformed mitotic spindle-like structures and condensed/unaligned chromosomes. Scale bars, 20 μm (a, b, d, and e) and 20 μm (c and f). (B) Whole-mount immunostaining of mitotic cells in *Tubg1*$^{+/+}$ (a) and *Tubg1*$^{-/-}$ (b–f) blastocysts. Blastocysts were triple-stained with FITC-conjugated anti-α-tubulin mAb (green), anti-pericentrin mAb (a centrosomal marker; red), and DAPI (blue). In *Tubg1*$^{+/+}$ mitotic cells (a), pericentrin was concentrated at both poles of the mitotic spindle. In arrested mitotic cells in *Tubg1*$^{-/-}$ blastocysts (b–f), the mitotic spindle was highly disorganized, while the spindle MTs did not appear to be dramatically destabilized. These disorganized spindles showed one or two pole-like foci of bundled MTs that were surrounded by condensed chromosomes. These foci did not always contain pericentrin. Scale bar, 5 μm.

When *Tubg2*$^{+/-}$ mice were interbred, wild-type (*Tubg2*$^{+/+}$), heterozygous (*Tubg2*$^{+/-}$), and homozygous mutant (*Tubg2*$^{-/-}$) mice were born normally at the expected Mendelian segregation ratio, judging from Southern blotting (Fig. 4B; Table 1). We confirmed by RT-PCR that TUBG2 mRNA became undetectable in the brain of *Tubg2*$^{-/-}$ mice (Fig. 4C). In sharp contrast to *Tubg1*$^{-/-}$ mice, both male and female *Tubg2*$^{-/-}$ mice developed and grew normally in the laboratory environment at least up to 2 years of age and showed no differences in weight, size, or reproductive ability. We examined hematoxylin-eosin-stained sections of various tissues of *Tubg2*$^{-/-}$ mice, but detected no significant histological abnormalities even in the brain (data not shown).

Expression of TUBG1 and TUBG2 in wild-type mice

To interpret the difference in phenotypes between Tubg1$^{-/-}$ and Tubg2$^{-/-}$ mice, information on the expression and distribution of the products of these genes,

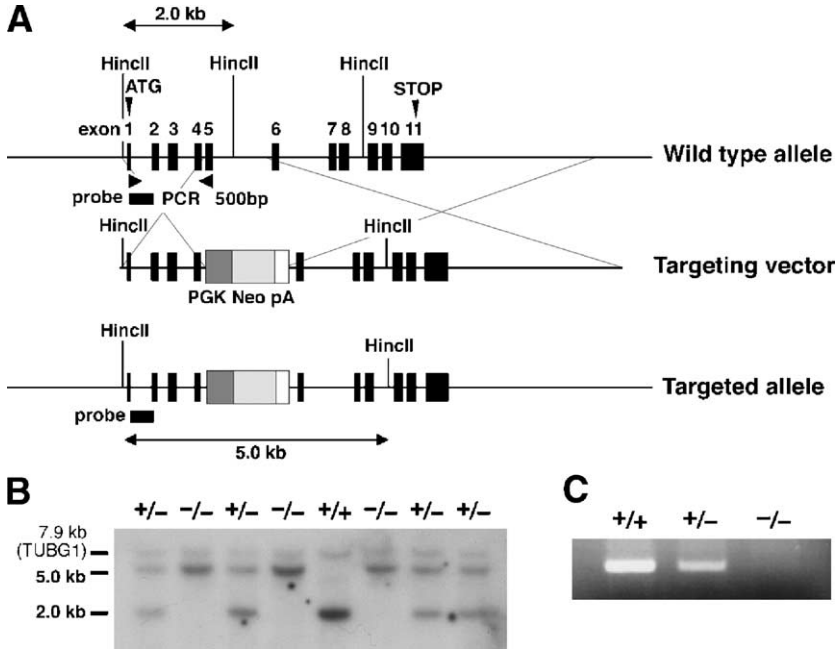

Fig. 4. TUBG2 gene knockout by homologous recombination in mice. (A) Restriction maps of the wild-type allele, the targeting vector, and the targeted allele of the mouse TUBG2 gene. Eleven exons (closed boxes) were identified, among which exons 1 and 11 contained the initiation and stop codons. The targeting vector contained the pgk neo cassette (PGK Neo) and a polyadenylation site (pA) in its middle portion to delete exon 5 in the targeted allele. The position of the 5′ probe for Southern blotting is indicated as a bar. Arrowheads show PCR primers used in C. (B) Genotype analyses by Southern blotting of *Hin*cII-digested genomic DNA from *Tubg2*$^{+/-}$ intercross littermates. Southern blotting with the 5′ probe yielded a 2.0-kb band from the wild-type allele and a 5.0-kb band from the targeted allele (see A). The 7.9-kb band detected faintly in all littermates would be attributed to the cross-hybridization of the probe to *Tubg1* allele (see Fig. 2A). (C) Loss of TUBG2 mRNA in the brain of *Tubg2*$^{-/-}$ mice examined by RT-PCR. Primers used for RT-PCR are shown in A.

especially, TUBG2, is prerequisite. As mentioned above, the lack of antibodies specific for TUBG1 and TUBG2 has hampered detailed analyses of these proteins. However, during the course of immunoblotting with a commercially available anti-γ-tubulin mAb that recognized TUBG1 and TUBG2 equally, we noticed that in the brain lysate of wild-type mice, the γ-tubulin-positive band was reproducibly split into two bands, upper and lower bands, and that only the upper band was detected in the lysates of other tissues such as the heart, liver, kidney, testis, etc. (Fig. 5B).

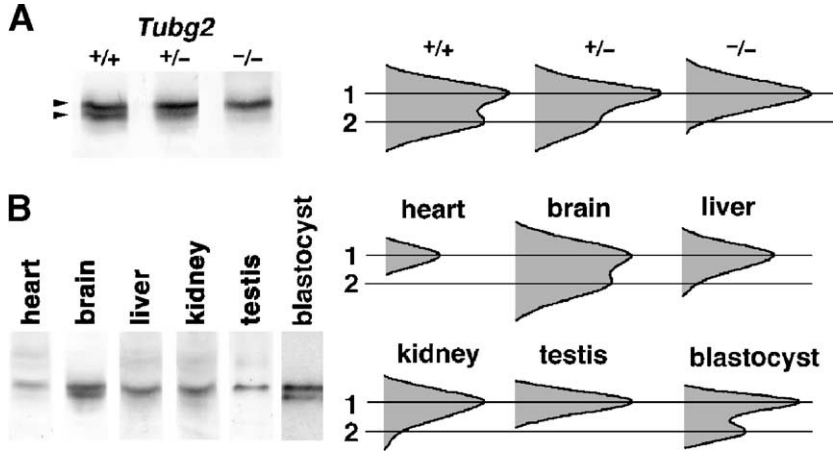

Fig. 5. Expression of TUBG2 at the protein level. (A) Distinction of TUBG2 from TUBG1 by immunoblotting. When the brain lysate of *Tubg2*$^{+/+}$ mice was immunoblotted with anti-γ-tubulin mAb that recognized TUBG1 and TUBG2 equally, the γ-tubulin-positive band was reproducibly split into two, upper and lower, bands (arrowheads). The lower band was decreased in intensity in *Tubg2*$^{+/-}$ brain and became undetectable in *Tubg2*$^{-/-}$ brain. The findings indicate that these bands represent TUBG1 and TUBG2, respectively. The densitometric scanning patterns of these bands are shown on the right, and the molar ratios of TUBG2(*2*)/TUBG1(*1*) were estimated to be ~0.8 (+/+), ~0.5 (+/–), and 0 (–/–). (B) Expression of TUBG2 in various tissues of wild-type mice. The whole lysates of the heart, brain, liver, kidney, testis, and blastocysts (10 embryos) obtained from wild-type mice were immunoblotted with anti-γ-tubulin mAb. TUBG2 was detected only in the brain and blastocysts. The densitometric scanning patterns are shown on the right. The molar ratio of TUBG2(*2*)/TUBG1(*1*) in blastocysts was estimated at ~0.7.

Interestingly, in the lysates of the *Tubg2*$^{-/-}$ brain, the lower band disappeared selectively, leaving a single γ-tubulin-positive band (Fig. 5A). Considering that TUBG2 is expressed in large amounts in the wild-type brain as shown by Northern blotting (Fig. 1C), it is safe to say that these upper and lower bands correspond to TUBG1 and TUBG2, respectively: this indicates that one can distinguish TUBG1 and TUBG2 by immunoblotting. As shown in Fig. 5, from the densitometric scanning of immunoblotted bands, we estimated that in the brain of wild-type mice, the molar ratio of TUBG2/TUBG1 is ~0.8.

Next, in order to discuss the relationship between TUBG1 and TUBG2 in cell division of wild-type early embryos, using this immunoblotting technique, we evaluated the expression levels of these two γ-tubulin isoforms in blastocysts (Fig. 5B). For this purpose, ~10 blastocysts were collected from the uterus of wild-type mice for each experiment and subjected to immunoblotting with anti-γ-tubulin mAb. Interestingly, very similar to the brain lysate, in wild-type blastocysts, TUBG2 was expressed at ~70% the level of TUBG1.

Finally, we examined the expression of TUBG2 in the wild-type brain in more detail (Fig. 6). We dissected manually the wild-type brain into the cerebral cortex, thalamus, striatum, hippocampus, and cerebellum, each of which was subjected to SDS–PAGE followed by immunoblotting with anti-γ-tubulin mAb: TUBG2 was detected in large amounts in all the portions of the brain except for the

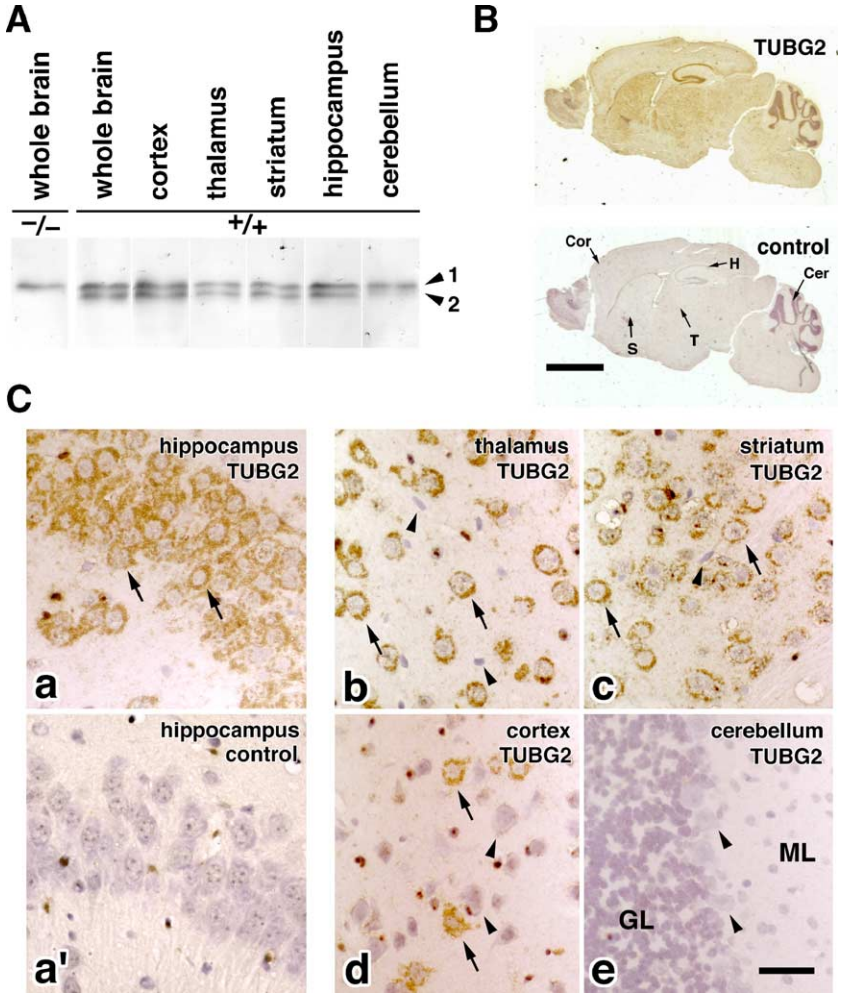

Fig. 6. Expression of TUBG2 in the wild-type brain. (A) Immunoblot analyses of TUBG1 (1) and TUBG2 (2) expression in various portions of the brain. Lysates from the whole brain of wild-type mice and manually dissected portions such as the cerebral cortex, thalamus, corpus striatum, hippocampus, and cerebellum (and the whole brain of *Tubg2*$^{-/-}$ mice as a control) were immunoblotted with anti-γ-tubulin mAb. Note that TUGB2 was expressed ubiquitously in the brain except for the cerebellum. (B) In situ hybridization on a sagittal section of the wild-type brain with a TUBG2-specific probe (upper panel) or non-labeled probe as a control (lower panel). These sections were counter-stained with hematoxylin to visualize nuclei in blue. TUBG2 mRNA signal (brown) was detected in especially large amounts in the cerebral cortex (Cor), thalamus (T), corpus striatum (S), hippocampus (H), but not detected in the cerebellum (Cer). (C) In situ hybridization images at higher magnification. In the CA3 subfield of the hippocampus (a), TUBG2 signals were intensely detected in all pyramidal cells (arrows) as compared to the control hybridization image (a′). In the thalamus (b) and corpus striatum (c), most cells with large nuclei were highly positive (arrows), whereas those with small nuclei were negative (arrowheads). In the cerebral cortex (d), the labeling was more heterogeneous depending on the cells. In the cerebellum (e), no significant signals were detected either from any cells in the granular (GL) and molecular layers (ML) or from Purkinje cells (arrowheads). Scale bars, 1 mm (B) and 20 μm (C).

cerebellum (Fig. 6A). In good agreement, in situ hybridization using a TUBG2-specific probe detected intensive signals from the cerebral cortex, thalamus, striatum, and hippocampus, but not from the cerebellum (Fig. 6B). At higher magnification, in the hippocampus, the granule cells in the dentate gyrus and the pyramidal cells of the hippocampus proper were highly positive (Figs. 6C, a and a′), and in the thalamus (Fig. 6C, b) and the striatum (Fig. 6C, c), most cells with large nuclei, but not those with small nuclei (which may correspond to neurons and glia cells, respectively), were heavily labeled. In the cerebral cortex, the labeling was more heterogeneous depending on cells (Fig. 6C, d). In contrast, in the cerebellum, no significant signals were detected from any cells in either the granular, molecular, or Purkinje cell layer (Fig. 6C, e).

Discussion

γ-Tubulin is thought to play a crucial role in regulating the organization of microtubule (MT)-based cytoskeletons in various eukaryotic cells (for reviews, see Moritz and Agard, 2001; Oakley, 2000; Schiebel, 2000). To date, in vitro analyses have been performed using mainly the γ-tubulin ring complex (γTuRC) isolated from *Xenopus* eggs or *Drosophila* embryos, and it is now widely accepted that γTuRC functions as a nucleation machinery for MT assembly to cap the MT minus-ends (reviewed in Gunawardane et al., 2000a; Job et al., 2003; Moritz and Agard, 2001; Schiebel, 2000; Wiese and Zheng, 1999). In contrast, our knowledge of the in vivo functions of γ-tubulin is still fragmentary, especially in vertebrates. Considering that in various species two (or three) closely related γ-tubulin isoforms were identified (Lajoie-Mazenc et al., 1996; Liu et al., 1994; Lopez et al., 1995; Ruiz et al., 1999; Tan and Heckmann, 1998; Wilson et al., 1997; Wise et al., 2000), as a next step, we should clarify the functions of γ-tubulin in vivo, especially the isoform-specific functions in detail.

In this study, we identified two closely related γ-tubulin isoforms, TUBG1 and TUBG2, in mice, and successfully generated mice lacking the expression of either TUBG1 or TUBG2: γ-tubulin isoforms corresponding to mouse TUBG1 and TUBG2 were already reported in humans (Wise et al., 2000) and were found in genomic database in chimpanzee, rat, and dog, but they have not yet been characterized. *Tubg1*$^{-/-}$ mice died before implantation due to mitotic arrest, whereas *Tubg2*$^{-/-}$ mice were born normally and exhibited no abnormality in either growth rate or fertility. Also in *Drosophila*, there are two γ-tubulin genes, γ*Tub23C* and γ*Tub37C* (Raynaud-Messina et al., 2001; Wilson et al., 1997). The γ*Tub23C* isoform is essentially ubiquitous and is required for viability and MT organization during mitosis and male meiosis (Sunkel et al., 1995). In contrast, the γ*Tub37C* isoform is involved in the meiosis of oocytes and nuclear proliferation in precellular embryos (Llamazares et al., 1999; Wilson and Borisy, 1998). Therefore, the present study revealed that the relationship between mouse *Tubg1* and *Tubg2* is completely different from that between *Drosophila* γ*Tub23C* and γ*Tub37C*. In good agreement, the phylogenetic tree analysis suggested that an ancestor γ-tubulin gene was duplicated independently for mouse/human *Tubg1*/*Tubg2* and *Drosophila* γ*Tub23C*/γ*Tub37C* pairs (see Fig. 1B).

The phenotypic abnormality observed in *Tubg1*$^{-/-}$ mice, i.e., the mitotic arrest around the morula/blastocyst stages, could be explained by the reported functions of γ-tubulin, the nucleation, and capping of MTs (Moritz et al., 1995; Wiese and Zheng, 2000; Zheng et al., 1995). Conversely, in mice (and probably also in humans), TUBG1 can be regarded as a conventional γ-tubulin that directly regulates the organization of MT-based cytoskeletons. The mitotic arrest in *Tubg1*$^{-/-}$ morula/blastocyst cells was very characteristic: the mitotic spindle was highly disorganized, while the spindle MTs did not appear to be dramatically destabilized. Usually, these disorganized spindles showed one or two pole-like foci of bundled MTs that were surrounded by condensed chromosomes. As γ-tubulin was reported to be concentrated at spindle poles in fertilized eggs of wild-type mice (Gueth-Hallonet et al., 1993; Palacios et al., 1993), it is reasonable to speculate that *Tubg1*$^{-/-}$ cells achieved mitosis normally until maternal TUBG1 was exhausted around the morula/blastocyst stages. Interestingly, when the expression of pericentrin A, which is directly involved in tethering γTuRC to centrioles (Dictenberg et al., 1998), was down-regulated by siRNA in human cultured cells, or when a peptide interfering with the association between pericentrin A and γTuRC was overexpressed, a very similar type of mitotic arrest was induced (Zimmerman et al., 2004). Consistently, in each arrested *Tubg1*$^{-/-}$ cell, there was one single pericentrin-positive focus, which showed no intimate spatial relationship with the pole-like foci of bundled MTs. Therefore, it would be safe to say that, in arrested *Tubg1*$^{-/-}$ cells, the TUBG1 deficiency suppressed the γ-tubulin-based nucleation around centrosomes, i.e., the astral formation, resulting in the formation of the characteristically deformed spindle-like structures surrounded by condensed chromosomes. This interpretation is consistent with recent observations that in the absence of centrosomes, spindle-like structures are formed based only on chromosomes, MTs, and MT motors (Heald et al., 1996; Karsenti and Vernos, 2001; Khodjakov et al., 2003; Walczak et al., 1998). Also in *C. elegans* and *Drosophila* cells in which the expression of γ-tubulin or a component of γTuRC was suppressed, the formation of mitotic spindles was reported to be severely affected, resulting in mitotic arrest (Barbosa et al., 2000; Bobinnec et al., 2000; Hannak et al., 2002; Sunkel et al., 1995). However, interestingly, the appearance/alignment of MTs and chromosomes in these cells was fairly distinct from those observed in *Tubg1*$^{-/-}$-arrested cells. For a better understanding of the functions of γ-tubulin in vivo,

especially as to how γ-tubulin is involved in spindle formation, this species-dependent difference should be examined in detail in future studies.

Tubg2$^{-/-}$ mice were born according to the Mendelian segregation ratio and grew at a normal rate, and both male and female *Tubg2*$^{-/-}$ offsprings were fertile. In this study, we failed to generate a TUBG1- or TUBG2-specific antibody, but based on the electrophoretic mobility, we found that TUBG2 (lower band) could be distinguished from TUBG1 (upper band) by immunoblotting with an anti-γ-tubulin mAb that recognized TUBG1 and TUBG2 equally. As TUBG1 and TUBG2 were nearly identical in sequence, the basis for this mobility difference was not clear. Of course, the possibility could not be completely excluded that the upper band was generated from the lower band through some modification such as ubiquitination (Starita et al., 2004), but taking it into consideration that the lower band was primarily detected in the wild-type brain expressing large amounts of TUBG2, and that this lower band of the brain disappeared completely in the *Tubg2*$^{-/-}$ mice, it would be reasonable to conclude that these upper and lower bands correspond to TUBG1 and TUBG2, respectively. With this technique, we found that in blastocysts of wild-type mice, TUBG2 was expressed in detectable amounts, at ~70% the amount of TUBG1. As shown in Fig. 1D, when FLAG-tagged TUBG2 cDNA was introduced into cultured Eph4 cells expressing endogenous TUBG1, FLAG-TUBG2 was recruited to and concentrated at centrosomes both in interphase and in mitotic cells. However, in *Tubg1*$^{-/-}$ blastocyst cells, whole-mount immunostaining with anti-γ-tubulin antibody did not identify any γ-tubulin (TUBG2)-positive foci (data not shown), though for each cell one pericentrin-positive focus occurred. Therefore, it suggests that TUBG2 is recruited to centrosomes only when TUBG1 is expressed and concentrated there, and that TUBG2 cannot rescue the TUBG1 deficiency in terms of cell division at least not in blastocyst cells, but further analyses are required at the cellular level in future studies.

Then, the question naturally arises as to what is the physiological functions of TUBG2. TUBG2 is expressed in large amounts in the brain of adult mice. Immunoblot analyses showed that the expression level of TUBG2 was nearly equal to that of TUBG1, although TUBG2 was expressed in less amounts in the cerebellum. In situ hybridization revealed that TUBG2 was expressed primarily in neurons, especially in large amounts in the thalamus, the striatum, and the hippocampus. Although conventional histochemical screening identified no abnormalities in *Tubg2*$^{-/-}$ mice, it is still possible that *Tubg2*$^{-/-}$ mice suffer from some defects in neuronal activities. Indeed, our preliminary observations suggested that *Tubg2*$^{-/-}$ mice appeared to exhibit peculiar behavioral deficits including abnormalities in circadian rhythm and the reaction to painful stimulations (our unpublished data). For a better understanding of the physiological functions of TUBG2 in the brain, TUBG2-specific antibodies must be generated to examine the subcellular distribution of TUBG2 in neurons in detail, and in parallel with such cell biological analyses, the behavior of *Tubg2*$^{-/-}$ mice should be examined systematically.

Acknowledgments

We thank all the members of our project of Solution Oriented Research in JST, and the ERATO Tsukita Cell Axis Project.

References

Barbosa, V., Yamamoto, R.R., Henderson, D.S., Glover, D.M., 2000. Mutation of a *Drosophila* gamma tubulin ring complex subunit encoded by discs degenerate-4 differentially disrupts centrosomal protein localization. Genes Dev. 14, 3126–3139.

Bobinnec, Y., Fukuda, M., Nishida, E., 2000. Identification and characterization of *Caenorhabditis elegans* gamma-tubulin in dividing cells and differentiated tissues. J Cell Sci. 113, 3747–3759.

Burns, R.G., 1995. Analysis of the gamma tubulin sequences: implications for the functional properties of gamma tubulin. J. Cell Sci. 108, 2123–2130.

Daunderer, C., Graf, R.O., 2002. Molecular analysis of the cytosolic *Dictyostelium* gamma-tubulin complex. Eur. J. Cell Biol. 81, 175–184.

Dictenberg, J.B., Zimmerman, W., Sparks, C.A., Young, A., Vidair, C., Zheng, Y., Carrington, W., Fay, F.S., Doxsey, S.J., 1998. Pericentrin and gamma-tubulin form a protein complex and are organized into a novel lattice at the centrosome. J. Cell Biol. 141, 163–174.

Doxsey, S.J., Stein, P., Evans, L., Calarco, P.D., Kirschner, M., 1994. Pericentrin, a highly conserved centrosome protein involved in microtubule organization. Cell 76, 639–650.

Felsenstein, J., 2003. PHYLIP (Phylogeny Inference Package), version 3.6a. Distributed by the author. Department of Genetics, University of Washington, Seattle.

Fulton, B.P., Whittingham, D.G., 1978. Activation of mammalian oocytes by intracellular injection of calcium. Nature 273, 149–151.

Furuse, M., Sasaki, H., Fujimoto, K., Tsukita, Sh., 1998. A single gene product, claudin-1 or -2, reconstitutes tight junction strands and recruits occludin in fibroblasts. J. Cell Biol. 143, 391–401.

Gueth-Hallonet, C., Antony, C., Aghion, J., Santa-Maria, A., Lajoie-Mazenc, I., Wright, M., Maro, B., 1993. gamma Tubulin is present in acentriolar MTOCs during early mouse development. J. Cell Sci. 105, 157–166.

Gunawardane, R.N., Lizarraga, S.B., Wiese, C., Wilde, A., Zheng, Y., 2000a. gamma-Tubulin complexes and their role in microtubule nucleation. In: Palazzo, R.E., Schatten, G.P. (Eds.), The Centrosome in Cell Replication and Early Development. Academic Press, San Diego, pp. 55–73.

Gunawardane, R.N., Martin, O.C., Cao, K., Zhang, L., Dej, K., Iwamatsu, A., Zheng, Y., 2000b. Characterization and reconstitution of *Drosophila* gamma-tubulin ring complex subunits. J. Cell Biol. 151, 1513–1524.

Hannak, E., Oegema, K., Kirkham, M., Gonczy, P., Habermann, B., Hyman, A.A., 2002. The kinetically dominant assembly pathway for centrosomal asters in *Caenorhabditis elegans* is gamma tubulin dependent. J. Cell Biol. 157, 591–602.

Heald, R., Tournebize, R., Blank, T., Sandaltzopoulos, R., Becker, P., Hyman, A., Karsenti, E., 1996. Self-organization of microtubules into bipolar spindles around artificial chromosomes in *Xenopus* egg extracts. Nature 382, 420–425.

Horio, T., Uzawa, S., Jung, M.K., Oakley, B.R., Tanaka, K., Yanagida, M., 1991. The fission yeast gamma tubulin is essential for mitosis and is localized at microtubule organizing centers. J. Cell Sci. 99, 693–700.

Job, D., Valiron, O., Oakley, B., 2003. Microtubule nucleation. Curr. Opin. Cell Biol. 15, 111–117.

Joshi, H.C., 1994. Microtubule organizing centers and gamma tubulin. Curr. Opin. Cell Biol. 6, 54–62.

Karsenti, E., Vernos, I., 2001. The mitotic spindle: a self-made machine. Science 294, 543–547.

Khodjakov, A., Copenagle, L., Gordon, M.B., Compton, D.A., Kapoor, T.M., 2003. Minus-end capture of preformed kinetochore fibers contributes to spindle morphogenesis. J. Cell Biol. 160, 671–683.

Komiya, T., Tanigawa, Y., Hirohashi, S., 1997. A large-scale in situ hybridization system using an equalized cDNA library. Anal. Biochem. 254, 23–30.

Laemmli, U.K., 1970. Cleavage of structural proteins during the assembly of the head of bacteriophage T4. Nature 227, 680–685.

Lajoie-Mazenc, I., Detraves, C., Rotaru, V., Gares, M., Tollon, Y., Jean, C., Julian, M., Wright, M., Raynaud-Messina, B., 1996. A single gamma tubulin gene and mRNA, but two gamma tubulin polypeptides differing by their binding to the spindle pole organizing centres. J. Cell Sci. 109, 2483–2492.

Liu, B., Joshi, H.C., Wilson, T.J., Silflow, C.D., Palevitz, B.A., Snustad, D.P., 1994. gamma Tubulin in *Arabidopsis*: gene sequence, immunoblot, and immunofluorescence studies. Plant Cell 6, 303–314.

Llamazares, S., Tavosanis, G., Gonzalez, C., 1999. Cytological characterisation of the mutant phenotypes produced during early embryogenesis by null and loss-of-function alleles of the γTub37C gene in *Drosophila*. J. Cell Sci. 112, 659–667.

Lopez, I., Khan, S., Sevik, M., Cande, W.Z., Hussey, P.J., 1995. Isolation of a full-length cDNA encoding *Zea mays* gamma tubulin. Plant Physiol. 107, 309–310.

Marschall, L.G., Jeng, R.L., Mulholland, J., Stearns, T., 1996. Analysis of Tub4p, a yeast gamma-tubulin-like protein: implications for microtubule-organizing center function. J. Cell Biol. 134, 443–454.

Mogensen, M.M., Malik, A., Piel, M., Bouckson-Castaing, V., Bornens, M., 2000. Microtubule minus-end anchorage at centrosomal and non-centrosomal sites: the role of ninein. J. Cell Sci. 113, 3013–3023.

Moritz, M., Agard, D.A., 2001. gamma-Tubulin complexes and microtubule nucleation. Curr. Opin. Struct. Biol. 11, 174–181.

Moritz, M., Braunfeld, M.B., Sedat, J.W., Alberts, B., Agard, D.A., 1995. Microtubule nucleation by gamma tubulin-containing rings in the centrosome. Nature 378, 638–640.

Moritz, M., Zheng, Y., Alberts, B.M., Oegema, K., 1998. Recruitment of the gamma-tubulin ring complex to *Drosophila* salt-stripped centrosome scaffolds. J. Cell Biol. 142, 775–786.

Moudjou, M., Bordes, N., Paintrand, M., Bornens, M., 1996. gamma-Tubulin in mammalian cells: the centrosomal and the cytosolic forms. J. Cell Sci. 109, 875–887.

Niwa, H., Yamamura, K., Miyazaki, J., 1991. Efficient selection for high-expression transfectants with a novel eukaryotic vector. Gene 108, 193–199.

Niwa, H., Miyazaki, J., Smith, A.G., 2000. Quantitative expression of Oct-3/4 defines differentiation, dedifferentiation or self-renewal of ES cells. Nat. Genet. 24, 372–376.

Oakley, B.R., 2000. gamma-Tubulin. In: Palazzo, R.E., Schatten, G.P. (Eds.), The Centrosome in Cell Replication and Early Development. Academic Press, San Diego, pp. 27–54.

Oakley, B.R., Akkari, Y.N., 1999. gamma-Tubulin at ten: progress and prospects. Cell Struct. Funct. 24, 365–372.

Oakley, C.E., Oakley, B.R., 1989. Identification of gamma tubulin, a new member of the tubulin superfamily encoded by *mipA* gene of *Aspergillus nidulans*. Nature 338, 662–664.

Oakley, B.R., Oakley, C.E., Yoon, Y., Jung, M.K., 1990. gamma Tubulin is a component of the spindle pole body that is essential for microtubule function in *Aspergillus nidulans*. Cell 61, 1289–1301.

Oegema, K., Wiese, C., Martin, O.C., Milligan, R.A., Iwamatsu, A., Mitchison, T.J., Zheng, Y., 1999. Characterization of two related *Drosophila* gamma-tubulin complexes that differ in their ability to nucleate microtubules. J. Cell Biol. 144, 721–733.

Palacios, M.J., Joshi, H.C., Simerly, C., Schatten, G., 1993. gamma Tubulin reorganization during mouse fertilization and early development. J. Cell Sci. 104, 383–389.

Raynaud-Messina, B., Debec, A., Tollon, Y., Gares, M., Wright, M., 2001. Differential properties of the two *Drosophila* gamma tubulin isotypes. Eur. J. Cell Biol. 80, 643–649.

Ruiz, F., Beisson, J., Rossier, J., Dupuis-Williams, P., 1999. Basal body duplication in *Paramecium* requires gamma tubulin. Curr. Biol. 9, 43–46.

Schiebel, E., 2000. gamma-Tubulin complexes: binding to the centrosome, regulation and microtubule nucleation. Curr. Opin. Cell Biol. 12, 113–118.

Schnackenberg, B.J., Khodjakov, A., Rieder, C.L., Palazzo, R.E., 1998. The disassembly and reassembly of functional centrosomes in vitro. Proc. Natl. Acad. Sci. U. S. A. 95, 9295–9300.

Shibata, H., Toyama, K., Shioya, H., Ito, M., Hirota, M., Hasegawa, S., Matsumoto, H., Takano, H., Akiyama, T., Toyoshima, K., Kanamaru, R., Kanegae, Y., Saito, I., Nakamura, Y., Shiba, K., Noda, T., 1997. Rapid colorectal adenoma formation initiated by conditional targeting of the *Apc* gene. Science 278, 120–123.

Sobel, S.G., Snyder, M., 1995. A highly divergent gamma-tubulin gene is essential for cell growth and proper microtubule organization in *Saccharomyces cerevisiae*. J. Cell Biol. 131, 1775–1788.

Spang, A., Geissler, S., Grein, K., Schiebel, E., 1996. gamma Tubulin-like *Tub4p* of *Saccharomyces cerevisiae* is associated with the spindle pole body substructures that organize microtubules and is required for mitotic spindle formation. J. Cell Biol. 134, 429–441.

Starita, L.M., Machida, Y., Sankaran, S., Elias, J.E., Griffin, K., Schlegel, B.P., Gygi, S.P., Parvin, J.D., 2004. BRCA1-dependent ubiquitination of gamma-tubulin regulates centrosome number. Mol. Cell. Biol. 24, 8457–8466.

Stearns, T., Kirschner, M., 1994. In vitro reconstitution of centrosome assembly and function: the central role of gamma tubulin. Cell 76, 623–637.

Stearns, T., Evans, L., Kirschner, M., 1991. gamma Tubulin is a highly conserved component of the centrosome. Cell 65, 825–836.

Strome, S., Powers, J., Dunn, M., Reese, K., Malone, C.J., White, J., Seydoux, G., Saxton, W., 2001. Spindle dynamics and the role of gamma tubulin in early *Caenorhabditis elegans* embryos. Mol. Biol. Cell 12, 1751–1764.

Sunkel, C.E., Gomes, R., Sampaio, P., Perdigao, J., Gonzalez, C., 1995. gamma Tubulin is required for the structure and function of the microtubule organizing centre in *Drosophila* neuroblasts. EMBO J. 14, 28–36.

Takahashi, M., Yamagiwa, A., Nishimura, T., Mukai, H., Ono, Y., 2002. Centrosomal proteins CG-NAP and kendrin provide microtubule nucleation sites by anchoring gamma-tubulin ring complex. Mol. Biol. Cell 13, 3235–3245.

Tan, M., Heckmann, K., 1998. The two gamma tubulin-encoding genes of the ciliate *Euplotes crassus* differ in their sequences, codon usage, transcription initiation sites and poly(A) addition sites. Gene 210, 53–60.

Tavosanis, G., Llamazares, S., Goulielmos, G., Gonzalez, C., 1997. Essential role for gamma tubulin in the acentriolar female meiotic spindle of Drosophila. EMBO J. 16, 1809–1819.

Vogel, J.M., Stearns, T., Rieder, C.L., Palazzo, R.E., 1997. Centrosomes isolated from Spisula solidissima oocytes contain rings and an unusual stoichiometric ratio of alpha/beta tubulin. J. Cell Biol. 137, 193–202.

Walczak, C.E., Vernos, I., Mitchison, T.J., Karsenti, E., Heald, R., 1998. A model for the proposed roles of different microtubule-based motor proteins in establishing spindle bipolarity. Curr. Biol. 8, 903–913.

Wiese, C., Zheng, Y., 1999. gamma Tubulin complexes and their interaction with microtubule-organizing centers. Curr. Opin. Struct. Biol. 9, 250–259.

Wiese, C., Zheng, Y., 2000. A new function for the gamma tubulin ring complex as a microtubule minus-end cap. Nat. Cell Biol. 2, 358–364.

Wilson, P.G., Borisy, G.G., 1998. Maternally expressed γ*Tub37CD* in *Drosophila* is differentially required for female meiosis and embryonic mitosis. Dev. Biol. 199, 273–290.

Wilson, P.G., Zheng, Y., Oakley, C.E., Oakley, B.R., Borisy, G.G., Fuller, M.T., 1997. Differential expression of two gamma tubulin isoforms during gametogenesis and development in *Drosophila*. Dev. Biol. 184, 207–221.

Wise, D.O., Krahe, R., Oakley, B.R., 2000. The gamma tubulin gene family in humans. Genomics 67, 164–170.

Wu, X., Palazzo, R.E., 1999. Differential regulation of maternal vs. paternal centrosomes. Proc. Natl. Acad. Sci. U. S. A. 96, 1397–1402.

Zheng, Y., Jung, M.K., Oakley, B.R., 1991. gamma Tubulin is present in *Drosophila melanogaster* and *Homo sapiens* and is associated with the centrosome. Cell 65, 817–823.

Zheng, Y., Wong, M.L., Alberts, B., Mitchison, T., 1995. Nucleation of microtubule assembly by a gamma tubulin-containing ring complex. Nature 378, 578–583.

Zimmerman, W.C., Sillibourne, J., Rosa, J., Doxsey, S.J., 2004. Mitosis-specific anchoring of gamma tubulin complexes by pericentrin controls spindle organization and mitotic entry. Mol. Biol. Cell 15, 3642–3657.